Available online at www.sciencedirect.com
ScienceDirect
Journal of Solid State Chemistry 179 (2006) 3229–3237
JOURNAL OF SOLID STATE CHEMISTRY
www.elsevier.com/locate/jssc

# Solvothermal synthesis and characterisation of $La_{1-x}A_xMnO_3$ nanoparticles

Carlos Vázquez-Vázquez*, M. Arturo López-Quintela

*Facultade de Química. Departamento de Química Física, Universidade de Santiago de Compostela, Santiago de Compostela, Spain*

Received 23 January 2006; received in revised form 20 April 2006; accepted 11 June 2006
Available online 27 June 2006

**Abstract**

The synthesis of $La_{1-x}A_xMnO_3$ ($A$ = Ca, Sr, Ba) nanoparticles in nonaqueous solvents has been studied. For this solvothermal procedure benzyl alcohol and acetophenone were chosen as reaction media. After this treatment in mild conditions a precipitate was obtained, which, however, can be annealed to the crystalline perovskite structure. Our results show that acetophenone is more suited to obtain the clean pervoskite phase than benzyl alcohol.


*Keywords:* Solvothermal synthesis; Nanoparticles; Lanthanum manganite; Non-aqueous synthesis

## 1. Introduction

The discovery of giant and colossal magnetorresistance in doped lanthanum manganite, $La_{1-x}A_xMnO_3$ ($A$ = Ca, Sr, Ba), thin films [1] and polycrystalline samples [2], respectively, was the starting point for a number of research studies related to those perovskites. Their interesting magnetic and magnetotransport properties are related to the mixed-valence of the manganese cations in the perovskite structure, due to the hopping of electrons between Mn(III) and Mn(IV) cations and the presence of cationic vacancies. Additionally, these manganites have also shown catalytic activity [3] and are interesting as cathode materials in solid oxide fuel cells [4].

Different synthetic procedures have been used for preparing these materials in order to study the influence of particle size on their properties, including conventional solid state reaction, coprecipitation [5], sol–gel [6] and molten salts reactions [7].

In the search of novel pathways for the synthesis of $La_{1-x}A_xMnO_3$ nanoparticles, hydrothermal methods have also been studied in some papers. Bernard et al. have prepared $La_{1-x}Sr_xMnO_{3+d}$ by using nitrate and acetate precursors in hydrothermal conditions, adding citric acid as complexing agent, and adjusting the pH with ammonia or tetramethyl ammonium hydroxide [8]. Zhu et al. have prepared $La_{0.5}Sr_{0.5}MnO_3$ and $La_{0.5}Ba_{0.5}MnO_3$ nanowires by adding potassium permanganate in alkaline medium to the metallic precursor [9]. Urban et al. have improved the synthetic conditions of the last procedure and were able to prepare $La_{0.5}Ba_{0.5}MnO_3$ single-crystalline nanocubes [10].

Nevertheless, the synthesis of $La_{1-x}A_xMnO_3$ nanoparticles in nonaqueous conditions (i.e. a solvothermal procedure) has not been yet explored. This novel synthetic procedure has been used by Niederberger et al. for preparing highly crystalline simple oxides as $TiO_2$ [11], $VO_2$, $WO_3$ [12], $Fe_2O_3$ [13] nanoparticles; as well as some few ternary oxides, such as $BaTiO_3$ and $SrTiO_3$ [14]. Here we report the successful solvothermal preparation of a series of doped and undoped lanthanum manganites: $La_{1-x}A_xMnO_3$ ($A$ = Sr, Ca, Ba; doping level: $x = 0.33$) and $LaMnO_3$, using either benzyl alcohol or acetophenone as solvents.

## 2. Experimental section

*Materials*: La(III) chloride, Mn(II) chloride, La(III) acetate hydrate, Ca(II) acetate monohydrate, Ba(II) acetate, Sr(II) acetate and Mn(III) acetate dihydrate were

*Corresponding author. Fax: +34 981 595012.
*E-mail address:* qfmatcvv@usc.es (C. Vázquez-Vázquez).

0022-4596/$ - see front matter © 2006 Elsevier Inc. All rights reserved.
doi:10.1016/j.jssc.2006.06.021

supplied by Sigma-Aldrich (Germany); Ca(II) chloride, by Merck KGaA (Germany); benzyl alcohol and acetophenone, by Fluka (Switzerland); Mn(II) methoxide, by Alfa-Aesar (Germany); La(III) isopropoxide and La(III) methoxyethoxide (10–12% in methoxyethanol), by Gelest (ABCR, Karlsruhe, Germany); Mn(III) acetylacetonate, by Strem Chemicals (USA). All the chemicals were stored in a glove box under Ar atmosphere.

*Synthesis*: All the syntheses were carried out in autoclaves Parr Acid Digestion Bombs with 23 or 45 mL Teflon cups. The temperatures ranged from 180 to 250 °C and the treatments lasted from 15 to 100 h, depending on the synthesis.

*Benzyl alcohol as solvent*: In a typical synthesis, the anhydrous metallic chlorides were dissolved separately in 1–2 g of ethanol (or directly in benzyl alcohol, as in sample B3) under mild stirring for 30 min. Afterwards, they were transferred to the Teflon vessel and filled up to $\frac{3}{4}$ its volume with benzyl alcohol. The mixture was stirred for 1–2 h before the autoclave was closed. All this procedure was carried out in the glove box. The solvothermal treatment at 200 °C for 2–3 days yields a white product that was centrifuged at 6500 rpm. Then, several washing-centrifugation steps were performed with 20 mL of ethanol ( × 2) and 20 mL of tetrahydrofuran (THF) ( × 2) before the powder was dried overnight at 100 °C. When Mn(II) methoxide was used as reagent, it was dissolved in 2 g of methanol.

*Acetophenone as solvent*: In a typical synthesis, the metallic acetates were dissolved directly in acetophenone under mild stirring for 30 min. Then, the mixture was transferred to the autoclave and after 15 min stirring it was closed. The solvothermal treatment was carried out at 200 °C for 15–20 h and a brown product was obtained. This product was centrifuged at 6500 rpm and, afterwards, washed and centrifuged several times with 15–20 mL of chloroform or methylene chloride ( × 3). Then, the sample was dried overnight at 100 °C.

For both solvents (benzyl alcohol and acetophenone), when the metallic acetates were used, a preliminary evaporation step at 120 °C was carried out in some cases in order to remove the water given by the hydrated acetates.

The experimental conditions of the different samples are summarised in Tables 1 and 2. All the samples prepared with benzyl alcohol as solvent will be labelled as B, while those prepared with acetophenone as A.

The dried precursors were then calcined at different temperatures ranging from 500 to 800 °C in order to crystallise the perovskite.

*Characterisation*: The samples were characterised structurally by X-ray powder diffraction (XRD) using a Bruker D8 diffractometer (CuKα radiation) in symmetric reflection. The diffractograms were compared with the PDF-2 database in order to identify the crystalline phases present in the samples. The amount of impurities was obtained qualitatively from the relative intensity of the main reflections of the several crystalline phases. The thermogravimetric measurements were carried out in a Perkin

Table 1
Experimental conditions of the samples prepared in benzyl alcohol

| Sample | La reagent | Mn reagent | [BzOH]/[Mn(II)] | $T$ (°C) | Time (h) |
|---|---|---|---|---|---|
| B1 | La(III) chloride | Mn(II) chloride | 80 | 200 | 89 |
| B2 | La(III) chloride | Mn(II) chloride | 40 | 200 | 89 |
| B3 | La(III) chloride | Mn(II) chloride | 80 | 200 | 62 |
| B4 | La(III) methoxyethoxide | Mn(II) methoxide | 798.6 | 250 | — |
| B5 | La(III) methoxyethoxide | Mn(II) methoxide | 776.6 | 180 | 24 |
| B6 | La(III) methoxyethoxide | Mn(II) methoxide | 789.4 | 200 | 17 |
| B7 | La(III) acetate hydrate | Mn(III) acetate dihydrate | 112.3 | 200 | 20 |
| B8 | La(III) acetate hydrate | Mn(III) acetate dihydrate | 589.7 | 200 | 14 |

Table 2
Experimental conditions of the samples prepared in acetophenone (all prepared at 200 °C)

| Sample | La reagent | Mn reagent | A reagent | [solvent]/[Mn(II)] | Time (h) |
|---|---|---|---|---|---|
| A1 | La(III) isopropoxide | Mn(III) acetylacetonate | — | 735.9 | 20.5 |
| A2 | La(III) acetate hydrate | Mn(III) acetate dihydrate | — | 815.1 | 16.5 |
| A3 | Idem | Idem | — | 115.9 | 20 |
| A4 | Idem | Idem | — | 511.0 | 14 |
| A5 | Idem | Idem | Ba(II) acetate | 344.9 | 19 |
| A6 | Idem | Idem | Sr(II) acetate | 299.2 | 18 |
| A7 | Idem | Idem | Ca(II) acetate dihydrate | 277.8 | 16.5 |
| A8 | Idem | Idem | Ba(II) acetate | 321.6 | 18 |
| A9 | Idem | Idem | Sr(II) acetate | 300.1 | 17.5 |

Elmer TGA 7 thermobalance under $N_2$ flow and with a scan rate of 10 °C/min. Transmission electron microscopy (TEM) images were taken with a Zeiss EM 912 Ω at an acceleration voltage of 120 kV. Samples were ground in a mortar and taken up in acetone. One droplet of the suspension was applied to a 400 mesh carbon-coated copper grid and left to dry in air. The infrared spectra were recorded in a Bruker IFS-66v, with a scanning resolution of 0.25 $cm^{-1}$. The magnetic measurements were performed in a Quantum Design SQUID from 5 to 350 K in field-cooling (FC) and zero-field-cooling (ZFC) conditions with an applied magnetic field of 1000 G.

## 3. Results and discussion

### 3.1. X-ray diffraction study

#### 3.1.1. Benzyl alcohol as solvent

These samples were labelled as "B" samples. The results are summarised in Tables 3 and 4, where it is indicated the predominant and the secondary crystalline phases obtained during the synthesis.

The samples B1, B2 and B3—prepared from the La(III) and Mn(II) chlorides—showed thick needles (thicker than several hundreds of nanometers) of LaOCl (PDF

Table 3
X-ray diffraction study of the samples prepared in benzyl alcohol

| Sample | Thermal treatment | Predominant phase | Secondary phases |
|---|---|---|---|
| B1_b, B2_b, B3_b | 600 °C 3 h | LaOCl | — |
| B4_a, B5_a | As prepared | $La(OH)_3$ | — |
| B5_b | 600 °C 3 h | Mixture of different $La_2O_2CO_3$ | $LaMnO_{3.15}$ |
| B6_b | 600 °C 3 h | Mixture of different La(III) carbonate and oxycarbones | |
| B6_c | Idem + 800 °C 3 h | $La_2O_3$ | $LaMnO_{3.15} + La(OH)_3$ |
| B7_b | 600 °C 6 h | $La(OH)_3$ | Tetragonal $La_2O_2CO_3 + LaMnO_{3.15}$ |
| B7_c | 700 °C 3 h | $La(OH)_3$ | $LaMnO_{3.15} + Mn_3O_4$ |
| B7_d | 500 °C 2 h + wash with HOAc + 700 °C 3 h | $LaMnO_{3.15}$ | $Mn_3O_4$ |
| B7_e | Wash with HOAc + 700 °C 3 h | $LaMnO_{3.15}$ | $Mn_3O_4$ |
| B8_b | 600 °C 6 h | Tetragonal $La_2O_2CO_3$ | $LaMnO_{3.15}$ |
| B8_c | 700 °C 3 h | $La(OH)_3$ | $LaMnO_{3.15} + La_2O_3$ |
| B8_d | 500 °C 2 h + wash with HOAc + 700 °C 3 h | $LaMnO_{3.15}$ | $La_2O_3 + Mn_2O_3$ |

Table 4
X-ray diffraction study of the samples prepared in acetophenone

| Sample | Thermal treatment | Predominant phase | Secondary phases |
|---|---|---|---|
| A1_b | 600 °C 3 h | $LaMnO_{3.15}$ | $La_2O_2CO_3$ |
| A1_c | Idem + 800 °C 3 h | $LaMnO_{3.15}$ | Unknown |
| A1_d | 600 °C 2 h + washing step + 600 °C 2 h | $LaMnO_{3.15}$ | $La_2O_2CO_3$ |
| A2_b | 500 °C 2 h | Amorphous | Hexagonal $La_2O_2CO_3$ |
| A2_c | Idem + washing step + 600 °C 3 h | $LaMnO_{3.15}$ | Amorphous |
| A2_d | Idem + 700 °C 3 h | $LaMnO_{3.15}$ | — |
| A3_b | 500 °C 2 h | Tetragonal $La_2O_2CO_3$ | |
| A3_c | 600 °C 6 h | $LaMnO_{3.15}$ | Tetragonal $La_2O_2CO_3$ |
| A3_d | 700 °C 3 h | $LaMnO_{3.15}$ | Hexagonal $La(OH)_3$ |
| A3_e | 500 °C 2 h + washing step + 700 °C 3 h | $LaMnO_{3.15}$ | Mixture of different $La_2O_2CO_3 + Mn_2O_3$ |
| A3_f | Washing step + 700 °C 3 h | Hexagonal $La(OH)_3$ | |
| A4_b | 500 °C 2 h | Tetragonal $La_2O_2CO_3$ | |
| A4_c | 600 °C 6 h | $LaMnO_{3.15}$ | Hexagonal $La(OH)_3$ + tetragonal $La_2O_2CO_3$ |
| A4_d | 700 °C 3 h | $LaMnO_{3.15}$ | Hexagonal $La_2O_2CO_3$ |
| A4_e | 500 °C 2 h + washing step + 700 °C 3 h | $LaMnO_{3.15}$ | $Mn_3O_4$ |
| A6_b | 500 °C 2 h | Tetragonal $La_2O_2CO_3$ | — |
| A6_c | 600 °C 3 h | $La_2O_3$ | Perovskite |
| A6_d | 700 °C 3 h | $La_{0.8}Sr_{0.2}MnO_3$ | Hexagonal $La(OH)_3$ |
| A7_b | 500 °C 2 h | $La_{0.6}Ca_{0.4}MnO_3$ | $La_2CO_5$ |
| A7_c | 600 °C 3 h | $La_{0.6}Ca_{0.4}MnO_3$ | Hexagonal $La_2O_2CO_3$ |
| A7_d | 700 °C 3 h | $La_{0.6}Ca_{0.4}MnO_3$ | Hexagonal $La_2O_2CO_3$ |
| A8_b | 500 °C 2 h | $BaCO_3$ Witherite | $La_2CO_5$ |
| A8_c | 600 °C 3 h | $BaCO_3$ Witherite | Perovskite + $La_2Co_5$ |
| A8_d | 700 °C 3 h | Perovskite | $La_2O_3$ + hexagonal $La(OH)_3$ |

card no. 8-477). So, the presence of chloride anions interferes with the synthesis of the manganite.

In the samples B4, B5 and B6—prepared from the La(III) and Mn(II) alkoxides—the range of temperatures was restricted. At 250 °C the pressure is higher than 80 bars and the rupture disk was broken. So, the other syntheses were carried out at 180 and 200 °C. The diffraction patterns of the as-prepared samples matched with hexagonal $La(OH)_3$ (PDF card no. 36-1481) and, after the calcination at 600 °C, a mixture of several lanthanum oxycarbonates ($La_2O_2CO_3$ or $La_2CO_5$) were obtained: tetragonal (type I; PDF card no. 23-320), monoclinic (type 1A; PDF card no. 23-322) and hexagonal (type II, PDF card no. 37-804). The presence of several types of oxycarbonates is in accordance with the reported transition temperatures for the tetragonal to monoclinic (at ca. 500 °C) and the monoclinic to hexagonal allomorphs (at ca. 525 °C).

In order to avoid the presence of oxycarbonates, an evaporation step at 150 °C was added to the synthesis. In this way, the low-boiling-point solvents (water, methoxyethanol and methanol) were removed from the mixture. However, the results were not satisfactory: a mixture of lanthanum carbonate and oxycarbonates was obtained up to 600 °C (sample B6_b) and, after calcination at 800 °C (sample B6_c), hexagonal $La_2O_3$ (PDF card no. 5-602) mixed with the distorted perovskite ($LaMnO_{3.15}$, PDF card no. 32-484) and hexagonal $La(OH)_3$ (PDF card no. 36-1481).

Depending on the Mn(IV) content, $LaMnO_{3+\delta}$ has two main deviations from the ideal cubic structure of the perovskite: for Mn(IV) contents below ca. 20% (i.e. for $\delta \leqslant 0.10$), the structure is orthorhombic (space group Pbnm), while for Mn(IV) contents above ca. 20% (i.e. for $\delta > 0.10$), a rhombohedric distortion is present (space group R-3c) [15]. These two structures are easy to identify because, in the case of the rhombohedrally-distorted structure, a splitting of the main reflection of the perovskite (at ca. 32.5°2$\theta$) is observed. In all the samples studied we have never observed this splitting; so, this is a clear indication that the samples have a low Mn(IV) content.

In the samples B7 and B8—prepared from the La(III) and Mn(III) acetates—both approaches were used: the direct synthesis at 200 °C (B7) and the synthesis with the evaporation step prior to the solvothermal treatment (B8). The results were more encouraging using the metal acetates but secondary phases were still present (as shown in Table 3). In some cases, small amounts of hausmannite ($Mn_3O_4$, PDF card no. 24-734) were observed after washing with diluted acetic acid. This can be related to the removal of lanthanum oxycarbonates from the solid phase during the washing step.

The fact that benzyl alcohol is slightly acidic in the presence of water ($pK_a = 15.2$) could be the reason for such a large amount of unwanted phases. So, a less acidic organic solvent was tried [16]: acetophenone has a $pK_a \sim 20$ in the alpha C–H position and also a high boiling point (202 °C).

*3.1.2. Acetophenone as solvent. Undoped lanthanum manganites*

These samples were labelled as "A" samples. The results were much better in this case and are summarised in Table 4.

In the samples of the series A1—prepared from the La(III) isopropoxide and Mn(III) acetylacetonate—the predominant phase is always the perovskite and the secondary phase has only ~15% of relative intensity for the sample calcined at 800 °C.

When the La(III) and Mn(III) acetates were used as starting materials (series A2), the results were even closer to our needs. In Fig. 1 it is shown the diffraction patterns of these samples, showing that at low calcinations temperatures (500 °C) the sample is mainly amorphous and also some reflections from hexagonal $La_2CO_5$ (type II, PDF card no. 37-804) are present. This sample was washed with diluted acetic acid in order to remove these oxycarbonates and then it was annealed at 600 °C (sample A2_c) and afterwards at 700 °C (sample A2_d). Pure lanthanum manganite was obtained in this case.

The crystallite size, $D_{hkl}$, of the samples prepared at 600 and 700 °C was calculated from the main reflection of the rhombohedrally-distorted perovskite by means of the Debye–Scherrer equation:

$$D_{110}(\text{Å}) = \frac{k \cdot \lambda}{\beta \cdot \cos\theta},$$

where $k$ is a shape factor which normally ranges between 0.9 and 1.0 (in our case, $k = 0.9$), $\lambda$ is the X-ray wavelength ($CuK\alpha_1$, $\lambda = 1.54060$ Å), and $\theta$ is the Bragg angle. $\beta$ is the difference in profile widths of broadened and standard samples (in our case, a silicon standard was used): $\beta = \beta_{\text{sample}} - \beta_{\text{standard}}$, being $\beta$ the integral breadth defined as

$$\beta = \frac{\text{Area}(CuK\alpha_1)}{\text{Intensity}(CuK\alpha_1)}.$$

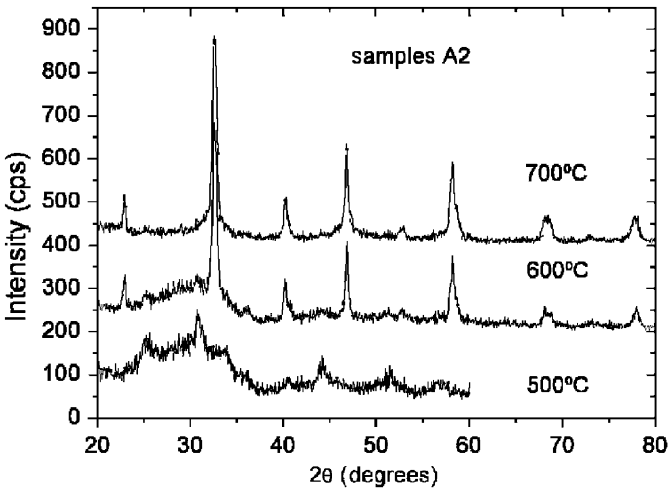


Fig. 1. X-ray diffractograms of the samples A2, prepared from the La(III) and Mn(III) acetates in acetophenone, calcined at several temperatures.

The individual fitting of the diffraction peaks were carried out using Gaussian profiles, and the crystallite size obtained for both samples was $D_{110} = 29$ nm.

Also in the samples of the series A3 the predominant phase was always the manganite; however, always a small amount of secondary phases were present (lanthanum hydroxide or oxycarbonates).

In order to remove the carbonates, the precursor was washed with diluted acetic acid just after preparation (sample A3_f). The calcination product in this case is only lanthanum hydroxide because the lanthanum oxide is transformed to hydroxide due to moisture [17].

The evaporation step for removing low-boiling-point solvents prior to the solvothermal treatment (samples A4) did not improve significantly the perovskite content, as compared with the samples without evaporation. However, in the case of the sample A4_e (annealed at 700 °C after a washing step with diluted acetic acid) the diffraction pattern matches well with the manganite, showing only two small broad bands (~3% of relative intensity, at ca. 29 and 36°2$\theta$ that can be assigned to hausmannite ($Mn_3O_4$, PDF card no. 24-734).

### 3.1.3. Acetophenone as solvent. Doped lanthanum manganites

The samples of the series A6, A7 and A8 correspond to doped lanthanum manganites. The nominal stoichiometries are $La_{0.67}Sr_{0.33}MnO_3$ for samples A6, $La_{0.67}Ca_{0.33}MnO_3$ for samples A7 and $La_{0.67}Ba_{0.33}MnO_3$ for samples A8. In these cases, neither evaporation step nor washing step was carried out.

For the samples calcined at 500 °C, it was always observed the presence of broad reflections of tetragonal lanthanum oxycarbonate (type I; PDF card no. 23-320) (sample A6_b), calcium carbonate (Calcite, PDF card no. 5-586) (sample A7_b) or barium carbonate (Witherite, PDF card no. 5-378) (sample A8_b) in coexistence with broad bands due to the poor crystallisation of the perovskite at this temperature.

When the calcinations temperature is increased, the samples crystallise better and, although the carbonates and oxycarbonates are still present at 600 °C, the manganite becomes the predominant phase at 700 °C. In the case of strontium-doped lanthanum manganite (sample A6_d), the sample calcined at 700 °C shows a very small amount of $La(OH)_3$ as secondary phase (2% of relative intensity) (Fig. 2). The diffractogram matches well with the X-ray powder pattern of $La_{0.8}Sr_{0.20}MnO_3$ (monoclinic, PDF card no. 40-1100). However, there are few patterns of the doped lanthanum manganites in the PDF-2 database and, as a consequence, the stoichiometry cannot be determined from X-ray diffraction. For the calcium-doped sample (A7_d), the presence of hexagonal $La_2CO_5$ (type II, PDF card no. 37-804) is more important (16% of relative intensity). In this case, the diffractogram matches well with $La_{0.6}Ca_{0.4}MnO_3$ (orthorhombic, PDF card no. 46-513). For the barium-doped sample (A8_d), the diffractogram matches well with a similar structure as the calcium-doped lanthanum manganite (no X-ray powder pattern was found in the PDF-2 database for the barium-doped lanthanum manganite) but the presence of secondary phases is higher.

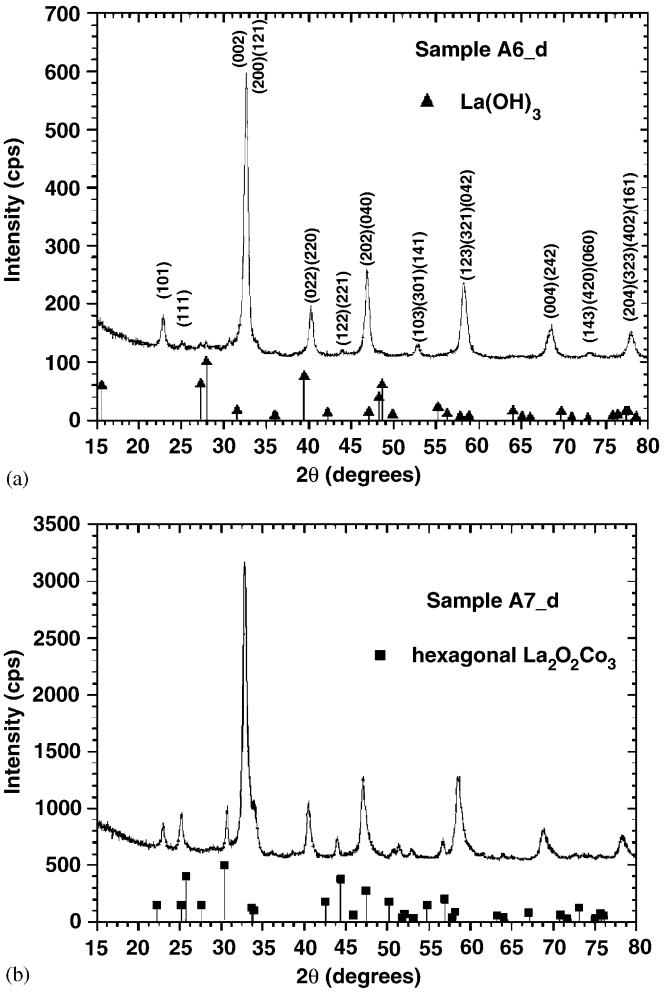


Fig. 2. X-ray diffractograms of the doped lanthanum manganites prepared from the metallic acetates in acetophenone and calcined at 700 °C: (a) sample A6_d, $La_{0.67}Sr_{0.33}MnO_3$; and (b) sample A7_d, $La_{0.67}Ca_{0.33}MnO_3$. The Miller indices from an orthorhombic perovskite structure have been included in the first graph. The main secondary phases are labelled in the two graphs: ▲ for $La(OH)_3$ in the first graph; and ■ for hexagonal $La_2O_2CO_3$, in the second one.

The crystallite size, $D_{110}$ of the strontium-doped lanthanum manganite sample prepared at 700 °C (A6_d) was obtained from the main reflection of the perovskite by means of the Debye–Scherrer equation, and is $D_{110} = 25$ nm.

All the as-prepared samples show crystalline materials, having some differences the diffraction patterns of the samples prepared in benzyl alcohol from those prepared in acetophenone. In Fig. 3 the X-ray diffraction pattern of sample A2_a, obtained when acetophenone is used as reaction medium is shown . The crystalline phase does not match with any crystalline material reported in the PDF-2

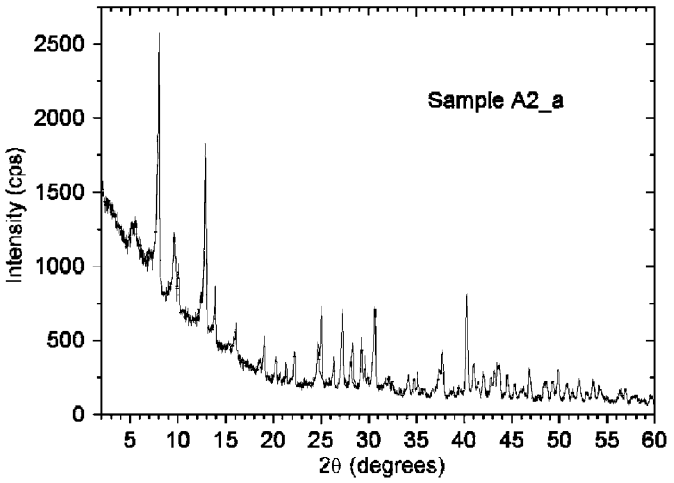


Fig. 3. X-ray diffractogram of the as-prepared sample A2_a, obtained from the metallic acetates in acetophenone.

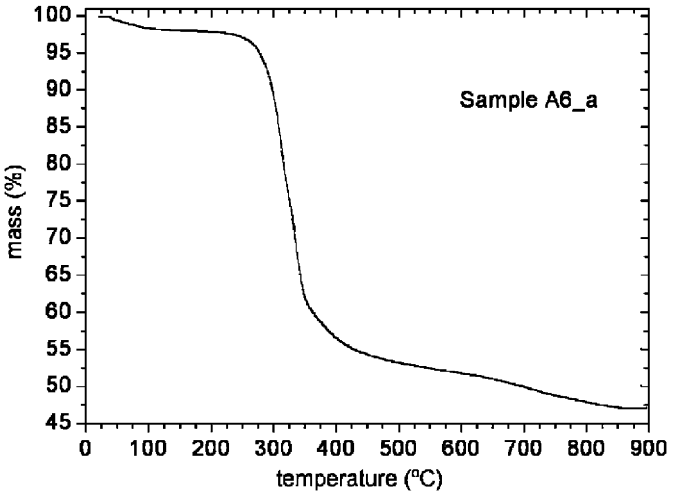


Fig. 4. Thermogravimetric curve of the as-prepared sample A6_a, obtained from the metallic acetates in acetophenone.

database. Because of the large number of reflections at low angles it is thought we have a nanocomposite. Similar results have been recently published by Pinna et al. for the solvothermal synthesis of yttria [18].

### 3.2. Thermogravimetric study

Fig. 4 depicts the thermogravimetric curve for the as-prepared sample A6_a, prepared in acetophenone and with the metallic acetates as starting reagents. Three steps can be observed:

(1) From room temperature to 150 °C (weight loss = 2%). This step is assigned to the moisture present in the sample.
(2) From 150 to 500 °C (weight loss = 44.9%). In this range of temperature, the acetates are decomposed into carbonates and oxycarbonates [19] . Additionally, the evaporation and/or decomposition of some remaining acetophenone can occur in this step. The decomposition of lanthanum acetate is reported to have the following stages in between 300 and 500 °C [19]:

$$La(CH_3CO_2)_3 \rightarrow LaCO_3(CH_3CO_2) + CH_3COCH_3,$$

$$LaCO_3(CH_3CO_2) \rightarrow \tfrac{1}{2}La_2(CO_3)_3 + \tfrac{1}{2}CH_3COCH_3,$$

$$La_2(CO_3)_3 \rightarrow La_2O_3.CO_2 + 2CO_2.$$

(3) From 500 to 900 °C (weight loss = 6.2%). In this step, the carbonates ($CaCO_3$, $BaCO_3$, $SrCO_3$ and $MnCO_3$) and oxycarbonates ($La_2O_2CO_3$) are decomposed to the corresponding oxides, by losing a $CO_2$ molecule. The formation of the perovskite occurs now by reaction between the different remaining oxides distributed all along the sample.

The same behaviour was observed for other as-prepared precursor.

### 3.3. Infrared study

The infrared spectra of the strontium-doped lanthanum manganite samples are shown in Fig. 5. The as-prepared sample (A6_a), at 200 °C, shows absorption bands almost identical to those of hydrated lanthanum acetate. Table 5 summarises the different assignments, taken from Karraker [20]. Some extra absorption bands are present due to the solvent (acetophenone).

Table 6 shows the assignments for the samples calcined at 500 and 600 °C. The main absorption bands match quite well with those of lanthanum hydroxycarbonate,

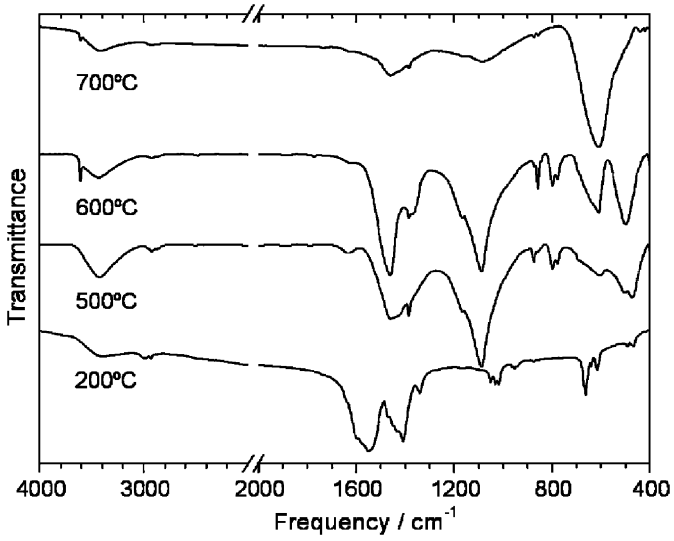


Fig. 5. Infrared spectra of the strontium-doped lanthanum manganite samples A6.

Table 5
Observed infrared absorption maxima of the as-prepared sample A6_a, and their assignments according to Karraker for hydrated lanthanum acetate [20]

| Observed frequencies ($cm^{-1}$) | Infrared absorption of $La(OAc)_3 \cdot 1.5$ $H_2O$ ($cm^{-1}$) | Band assignments |
|---|---|---|
| 3385 | 3360 | O–H stretch ($H_2O$) |
| 3003 | | C–H stretch of the aromatic ring |
| 2976 | | Asymmetric C–H stretch of the $CH_3$ group |
| 2929 | | Symmetric C–H stretch of the $CH_3$ group |
| 1597 | | C = C stretch aromatic ring |
| 1549 | 1555 | $-CO_2^-$ asymmetric stretch |
| 1451 | 1445 | $-CO_2^-$ symmetric stretch |
| 1408 | 1410 | $CH_3$ asymmetric bend |
| 1339 | 1346, 1332 | $CH_3$ symmetric bend |
| 1051, 1032-1016 | 1049, 1015 | $CH_3$ rocking |
| 950 | 938, 930 | C–C stretch |
| 663 | 663, 645 | OCO bend |
| 615, 490, 467 | 614, 467 | $-CO_2^-$ rocking |

Table 6
Observed infrared absorption maxima of the samples calcined at 500 and 600 °C (samples A6_b and A6_c), and their corresponding assignments

| Observed frequencies ($cm^{-1}$) Sample calcined at 500 °C | Observed frequencies ($cm^{-1}$) Sample calcined at 600 °C | Band assignments |
|---|---|---|
| | 3609 | $\nu_{s1}$ $OH^-$ |
| 3425 | 3438 | $\nu_{s2}$ $OH^-$ |
| 1632 | 1620 | HOH bend |
| 1460, 1427 | 1461, 1370 | $\nu_3$ $CO_3^{2-}$ |
| 1087 | 1087 | $\nu_1$ $CO_3^{2-}$ |
| 874 | 873 | $\nu_2$ $CO_3^{2-}$ |
| 798, 778 | 798, 778 | $\nu_4$ $CO_3^{2-}$ |
| 603 | 608 | Perovskite (Mn–O stretch) |
| 503, 472 | 497 | Cubic $La_2O_3$ (La–O stretch) |

$La(CO_3)OH$ [21], and lanthanum oxycarbonates, $La_2O_2CO_3$ [22]. In the sample calcined at 600 °C, the signal at 1370 $cm^{-1}$ points out the presence of the monoclinic or tetragonal polymorphs of the oxycarbonates [22].

The band at 1630 $cm^{-1}$ is due to the water bending mode [23], suggesting the presence of both hydroxide ions and molecular water.

The presence of an absorption band at 470–500 $cm^{-1}$ could be related to the existence of the cubic $La_2O_3$ [24,25]. This oxide is only stable in a short temperature range, from 500 to 600 °C. Above 620 °C it is reported to transform into the more stable hexagonal polymorph [26].

Additionally, some remaining absorption bands, present at 2850–2925 $cm^{-1}$, are due to the acetophenone or some decomposition products of this solvent.

In the sample calcined at 700 °C, there are still some carbonates because of the presence of the absorption bands at 1459 and 1082 $cm^{-1}$. However, the main absorption is located at 609 $cm^{-1}$ and it is assignable to the metal-oxygen stretching in the perovskite [27].

## 4. TEM study

The TEM micrographs of the as-prepared undoped lanthanum manganite (sample A2_a, where acetophenone

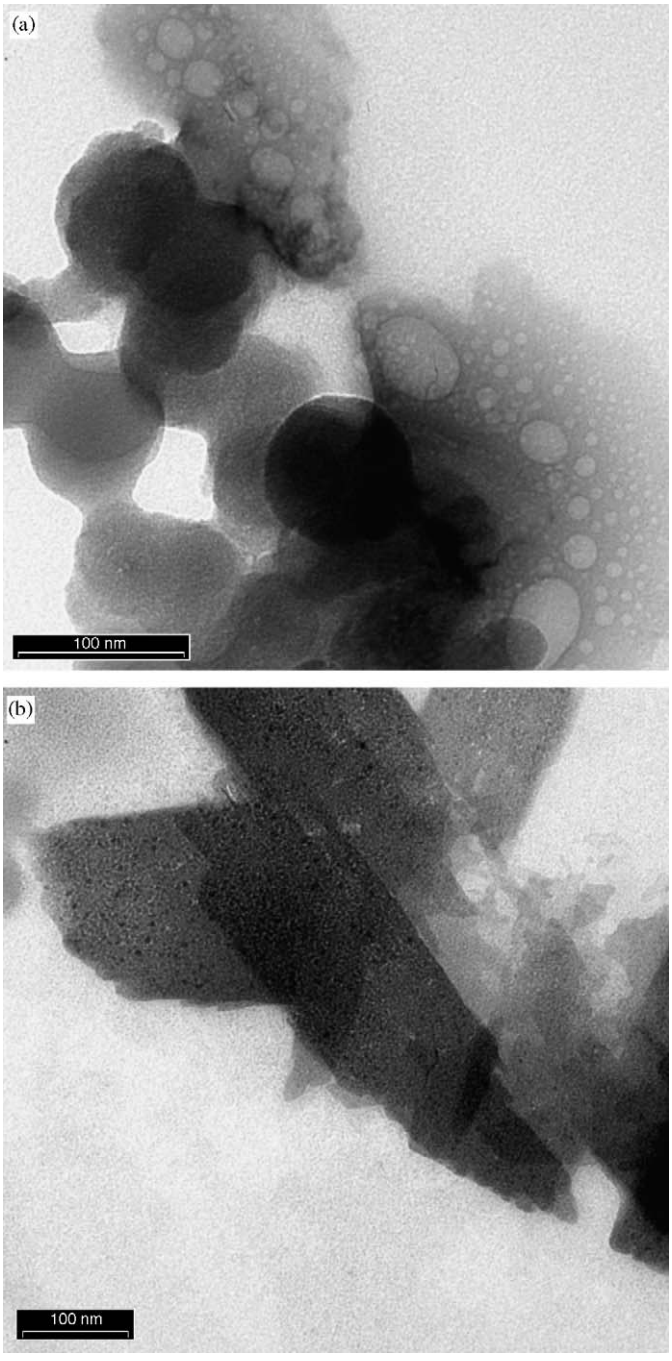


Fig. 6. Transmission electron micrographs of the undoped lanthanum manganites, prepared in acetophenone (sample A2_a), showing the different morphologies obtained (bar = 100 nm).

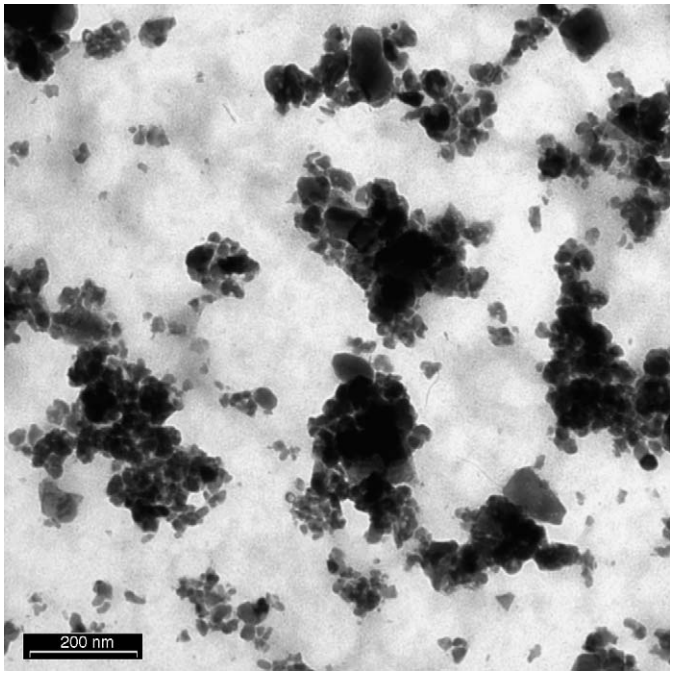


Fig. 7. Transmission electron micrograph of the undoped lanthanum manganites calcined at 600 °C (sample A2_c) (bar = 200 nm).

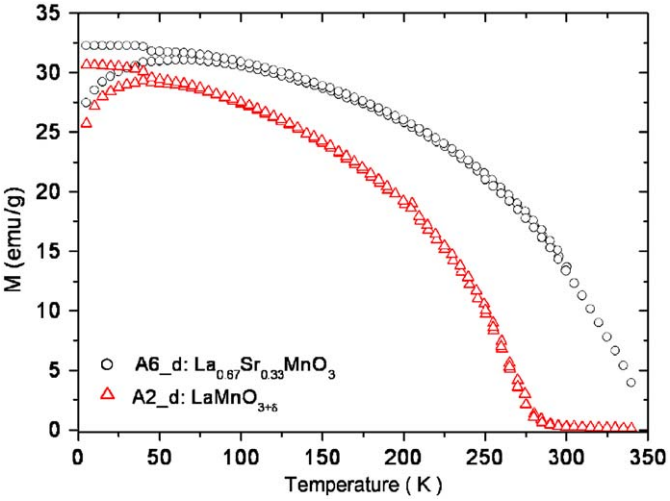


Fig. 8. Magnetisation curves as a function of the temperature for the undoped and strontium-doped lanthanum manganites calcined at 700 °C: samples A2_d and A6_d, respectively.

was used as solvent), are shown in Fig. 6. As it can be observed, the material presents a large variety of morphologies: elongated pieces, porous structures and quasi-spherical particles (Fig. 6a) and planar structures with some small particles (ca. 5 nm) adsorbed to them (Fig. 6b). The precursor is amorphous, as detected by X-ray diffraction; so, an annealing step is required for crystallising the perovskite. When this precursor is annealed at 600 °C for 3 h (sample A2_c), the sample starts to crystallise into nanoparticles with sizes ranging from 20 to 100 nm (Fig. 7). The particles are forming larger aggregates of several hundreds of nanometers in size, coming from the collapse of the original as-prepared sample.

In the case of the sample A6_d ($La_{0.67}Sr_{0.33}MnO_3$, calcined at 700 °C for 3 h), the nanoparticle size is, in average, a little larger than in the previous case and it ranges from 30 to 100 nm. The aggregation is still present.

## 5. Magnetic study

The magnetisation vs. temperature curves of the samples calcined at 700 °C A2_d ($LaMnO_{3+\delta}$) and A6_d ($La_{0.67}Sr_{0.33}MnO_3$) are shown in Fig. 8. The magnetisation were measured at an applied magnetic field, $H$, of 1000 Oe. The samples show a typical ferromagnetic behaviour. The Curie temperature, $T_C$, is obtained from the minimum of the first derivative of the magnetisation vs. temperature. For the sample A2_d, the value obtained for the ferromagnetic-to-paramagnetic transition is $T_C = 265$ K. More difficulties are found for the sample A6_d because of the lack of points above room temperature; however, the minimum in the first derivative has to be slightly above 350 K.

The inverse susceptibility, $\chi^{-1}$, vs. temperature indicate Curie–Weiss behaviour in the paramagnetic region [28]:

$$\text{Curie}-\text{Weiss law}: \chi = \frac{C}{T-\theta_p} \Rightarrow$$

$$\chi^{-1} = -\frac{\theta_p}{C} + \frac{1}{C}\cdot T,$$

where $C$ is the Curie constant and $\theta_p$ is the Weiss temperature.

From the linear fit in the paramagnetic region of sample A2_d we can obtain the value of the Weiss temperature, $\theta_p = 258 \pm 4$ K, and the Curie constant, $C$. This value is smaller than the Curie temperature, $\theta_p < T_C$, and can be related to the failure to reach a magnetisation corresponding to full ferromagnetic alignment of all Mn. So, it appears to signal either retention of some antiferromagnetic domains or a small antiferromagnetic component in the matrix [29].

From the value of the Curie constant it can be obtained the effective magnetic moment $\mu_{eff}$ [28]:

$$C = \frac{N\cdot\mu_{eff}^2}{3k_B},$$

where $N$ is the number of magnetic moments per mole and $k_B$ is the Boltzmann constant.

The value obtained for the sample A2_d is $\mu_{eff} = 4.573 \pm 0.017\mu_B$, where $\mu_B$ is the Bohr magneton. This value is between the calculated for spin-only moments on the Mn atoms: $\mu_{eff} = 4.90\mu_B$ for Mn(III) and $\mu_{eff} = 3.87\mu_B$ for Mn(IV). From this result, the amount of Mn(IV) and Mn(III) present in the sample can be obtained and, as a consequence, the oxygen stoichiometry of the perovskite $LaMnO_{3+\delta}$. In this case, there is a $31.7 \pm 1.7\%$ of Mn(IV) and, then, $\delta = 0.16$. However, this value can be

subjected to some error due to the small range of temperatures measured above the Curie temperature.

## 6. Conclusions

We have studied the synthesis of $La_{1-x}A_xMnO_{3+\delta}$ ($A$ = Ca, Sr, Ba) nanoparticles in nonaqueous solvents, trying to find the best conditions (metallic precursors, solvothermal temperature, solvent, annealing temperature). Acetophenone has proven to be a suitable solvent for the synthesis of the perovskite; however, in some cases, small amounts of secondary phases are also present. In all the cases, an annealing step is required after the solvothermal treatment in order to crystallise the perovskite. $La_{0.67}Sr_{0.33}MnO_{3+\delta}$ sample prepared in acetophenone (A2_d) shows a ferromagnetic behaviour and an effective magnetic moment of $\mu_{eff} = 4.573 \pm 0.017\mu_B$. From the magnetic measurements, the stoichiometry was estimated to be $La_{0.67}Sr_{0.33}MnO_{3.16}$.

## Acknowledgments

Carlos Vázquez-Vázquez wants to thank the Max–Planck Society for financial support (D.-B.K.). Markus Niederberger and Markus Antonietti are acknowledged for helpful discussion and lab facilities. Rona Pitschke is also acknowledged for the TEM measurements.

## References

[1] S. Jin, T.H. Tiefel, M. McCormack, R.A. Fastnacht, R. Ramesh, L.H. Chen, Science 264 (1994) 413.
[2] H.L. Ju, J. Gopalakrishnan, J.L. Peng, Q. Li, G.C. Xiong, T. Venkatesan, R.L. Greene, Phys. Rev. B 51 (1995) 6143.
[3] A. Hammouche, E. Siebert, A. Hammou, M. Kleitz, J. Electrochem. Soc. 138 (1991) 1212.
[4] S.J. Skinner, Fuel Cells Bull. 4 (2001) 6.
[5] I. Maurin, P. Barboux, Y. Lassailly, J.P. Boilot, Chem. Mater. 10 (1998) 1727.
[6] C. Vázquez-Vázquez, M.C. Blanco, M.A. López-Quintela, R.D. Sánchez, J. Rivas, S.B. Oseroff, J. Mater. Chem. 8 (1998) 991.
[7] C. Ciaravino, R. Lyonnet, J.P. Scharff, B. Durand, J.P. Deloume, J. High Temp. Mater. Proc. 3 (1999) 269.
[8] C. Bernard, C. Laberty, F. Ansart, B. Durand, Ann. Chim. Sci. Mat. 28 (2003) 85;
A. Barnabe, M. Gaudon, C. Bernard, C. Laberty, B. Durand, Mater. Res. Bull. 39 (2004) 725.
[9] D. Zhu, H. Zhu, Y. Zhang, Appl. Phys. Lett. 80 (2002) 1634;
D. Zhu, H. Zhu, Y.H. Zhang, J. Phys. Condens. Matter 14 (2002) L519.
[10] J.J. Urban, L. Ouyang, M.-H. Jo, D.S. Wang, H. Park, Nano Lett. 4 (2004) 1547.
[11] M. Niederberger, M.H. Bartl, G.D. Stucky, Chem. Mater. 14 (2002) 4364.
[12] M. Niederberger, M.H. Bartl, G.D. Stucky, J. Am. Chem. Soc. 124 (2002) 13642.
[13] M. Niederberger, F. Krumeich, K. Hegetschweiler, R. Nesper, Chem. Mater. 14 (2002) 78.
[14] M. Niederberger, G. Garnweitner, N. Pinna, M. Antonietti, J. Am. Chem. Soc. 126 (2004) 9120.
[15] A. Wold, R.J. Arnott, J.B. Goodenough, J. Appl. Phys. 29 (1958) 387.
[16] F.M. Menger, M. Ladika, J. Am. Chem. Soc. 109 (1987) 3145.
[17] M.P. Rosynek, D.T. Magnuson, J. Catalysis 46 (1977) 402.
[18] N. Pinna, G. Ganweitner, P. Beato, M. Niederberger, M. Antonietti, Small 1 (2005) 112.
[19] K.C. Patil, G.V. Chandrashekhar, M.V. George, C.N.R. Rao, Can. J. Chem. 46 (1968) 257.
[20] D.G. Karraker, J. Inorg. Nucl. Chem. 31 (1969) 2815.
[21] R. Aumont, C. R. Acad. Sci. Paris Série C 272 (1971) 314.
[22] S. Irusta, L.M. Cornaglia, E.A. Lombardo, Mater. Chem. Phys. 86 (2004) 440.
[23] N. Imanaka, T. Masui, Y. Kato, J. Solid State Chem. 178 (2005) 395.
[24] D.B. Faithful, S.M. Jonson, I.J. Mc Colm, Rev. Chim. Min. 10 (1973) 291.
[25] A.A. Filippova, A.A. Davydov, Y.M. Shchekochikhin, Izv. Sib. Otd. An. Khim. 1 (1976) 73.
[26] G. Brauer, E. Mohr-Rosenbaum, Z. Anorg. Allg. Chem. 394 (1972) 301.
[27] G.V. Subba Rao, C.N.R. Rao, J.R. Ferraro, Appl. Spectrosc. 24 (1970) 436.
[28] A.H. Morrish, The Physical Principles of Magnetism, IEEE Press, New York, 2001.
[29] J. Töpfer, J.B. Goodenough, Chem. Mater. 9 (1997) 1467.